

# BARC surface property matching for negative-tone development of a conventional positive-tone photoresist

Douglas J. Guerrero, Vandana Krishnamurthy, Daniel M. Sullivan

Brewer Science, Inc., 2401 Brewer Drive, Rolla, MO 65401, USA

## ABSTRACT

The main properties controlling a successful negative-tone development (NTD) process include surface energy of the BARC or silicon hardmask, reflectivity control, and type of spin-on carbon (SOC) layer utilized. In this paper, we studied the BARC and silicon-containing hardmask properties needed to achieve successful NTD of a conventional positive-tone photoresist. The surface energy mismatch between BARC and silicon-containing hardmask poses challenges for patterning dense structures. Interaction of the SOC layer and the photoresist was observed, even with the silicon hardmask film present in between these two layers. Strict reflectivity elimination does not guarantee a successful outcome, rather precise control of reflectivity is required to enhance the overall lithographic process.

**Keywords:** multilayer, NTD, surface energy

## 1. INTRODUCTION

New patterning techniques always present a new set of challenges that material developers must overcome to allow for adoption of new processes. The recent work on negative-tone developing (NTD) of conventional positive-tone ArF photoresists by organic solvents is not an exception<sup>1-3</sup>. This technique uses higher-contrast light-field imaging to produce exceptional contact hole and line space patterns<sup>4</sup>. Bottom anti-reflective coatings (BARCs) are still required in the NTD process to minimize substrate reflection, enhance resolution, and improve photoresist adhesion to substrate.

Changing the developer used does not change the reflectivity control of a BARC, but it does pose challenges to the adhesion of the photoresist, especially when the BARC is a spin-on silicon hardmask. The solvents used in the NTD process interact differently with the BARC-photoresist interface than the typical waterborne developer. Chemical mismatching at the BARC-resist interface can permit the solvent to penetrate and topple features. In addition, while standard positive-tone development (PTD) leaves behind a hydrophobic (protected) resist, NTD removes the protected resist, leaving a more hydrophilic resist on the substrate. Most underlayers used in current processes, particularly those with high silicon content, have been developed to match a more hydrophobic resist. As a consequence of this polarity switch, mismatch of surface energies between layers occurs which can be responsible for line collapse. Figure 1 shows a generic ArF photoresist structure<sup>5</sup> before and after exposure and post-exposure bake (PEB) and their corresponding property changes occurring during this process.

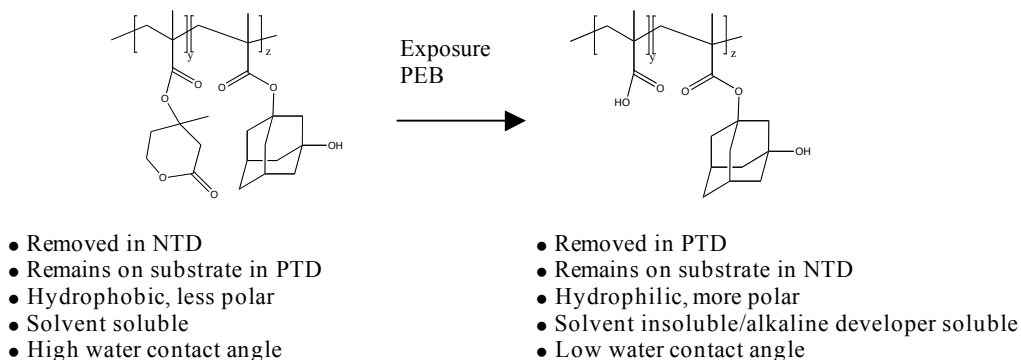


**Figure 1.** Structure and properties of an ArF resist before and after exposure and PEB.

D.J. Guerrero, V. Krishnamurthy, D.M. Sullivan, "BARC surface property matching for negative-tone development of a conventional positive-tone photoresist," *Proceedings of SPIE*, vol. 7972, 2011, in press.

© 2011 Society of Photo-Optical Instrumentation Engineers. One print or electronic copy of this preprint may be made for personal use only. Systematic reproduction and distribution, duplication of any material in this paper for a fee or for commercial purposes, or modification of the content of the paper are prohibited.

Previously, we have shown that a conventional organic BARC coating between the hardmask and photoresist provides the correct surface for resist adhesion in NTD<sup>6</sup> and could potentially be used as a solution to the mismatch of surface energies. However, from a processing point of view, direct patterning on a silicon hardmask coated on top of a carbon-rich layer (a spin-on carbon [SOC] layer) is desirable. In this paper we have investigated the effects that surface energy, film thickness, reflectivity, and pH of SOC underlayers have on lithographic performance. The stacks used in this evaluation were a simple two-layer stack (BARC/resist on silicon) and a multilayer stack, as illustrated in Figure 2.



**Figure 2.** Multilayer stack used in this study.

## 2. METHODOLOGY

### 2.0 General

Polymers containing 25-35% silicon were prepared by condensation of various siloxane monomers and were dissolved in PGME/PGMEA solvent to a nominal thickness of 30-40 nm. Film thickness on a silicon substrate was measured with a WS-LSE Gaertner ellipsometer. Ethyl lactate and negative-tone developer were used as stripper solvents to determine the minimum temperature required for baking the BARC while maintaining solvent resistance after coating and curing. The solvent was allowed to puddle on the film for 20 seconds and spin dried. The film thickness was compared before and after solvent contact. Most films were sufficiently cured to avoid intermixing at temperatures of 175°C or higher. Optical constants  $n$  and  $k$  were measured at 193 nm using a M2000 Woollam variable-angle spectroscopic ellipsometer.

### 2.1 Contact angle measurements

All silicon hardmasks were coated on a silicon substrate prior to contact angle measurements. The films were coated and baked on silicon wafers at 205°C. The measurements were done in an AST Products VCA Optima system under static conditions. The results are reported here are for static contact angle (SCA) using water.

### 2.2 Lithography

Samples were screened by patterning 65-nm S/130-nm P using 0.85NA, dipole illumination, and 0.91/0.71 sigma. FN-DP001 developer was used for 30 seconds with 10-second rinses with FN-RP002. Samples that did not show line collapse at this CD were further screened in a 1900i immersion scanner. The resists, developer, and rinse solvents used were manufactured by FujiFilm Electronic Materials (FFEM).

## 3. DATA AND RESULTS

### 3.1 Effect of contact angle on lithographic performance

Trench or contact hole patterning using an organic BARC can be easily achieved with the NTD process. For example, we have been able to pattern 45-nm CH/90-nm pitch on ARC<sup>®</sup>133 coating and 40-nm trenches/80-nm pitch on ARC<sup>®</sup>29SR coating (Figure 3). Contact hole patterning was achieved by using the double-trench-patterning technique in which two lines were exposed perpendicular from each other and followed by a single development process.



**Figure 3.** 45-nm CH/90-nm pitch (left) and 40-nm trenches/90-nm pitch (right) patterned on organic BARC using NTD.

While patterning on organic BARC is easily achieved, the overall lithographic performance is directly related to the surface energy of the BARCs used. In this study, three organic BARCs having varying contact angles were compared. The contact angle of the resist used after exposure and PEB was found to be 59°. The lithographic performance of each BARC was determined by calculating their underexposure margin. The underexposure margin is the exposure range from dose to size (65-nm trenches) to the line collapse point. In NTD, the lower the dose the larger the printed trench is. At the lowest doses, the space between the trenches becomes very small and the lines collapse. The relationship between the SCA of the BARCs used and the underexposure margin is shown in Figure 4 below. The underexposure margin is an important parameter because it allows the NTD process user to print a variety of pitches under an optimum dose target. In this case, a large underexposure margin is better.

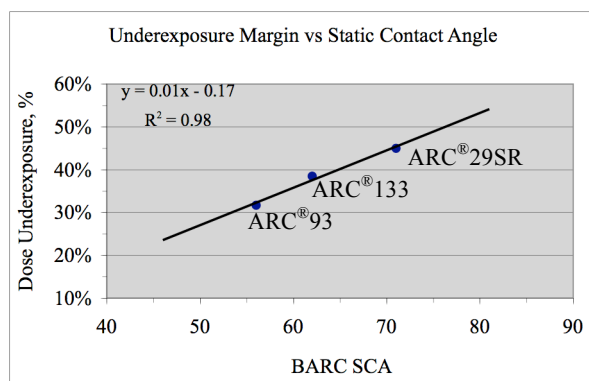


**Figure 4.** Relationship between BARC contact angle and underexposure margin.

This relationship must be taken with caution, as there are obviously other factors that can play significant roles, such as chemical compatibility of the individual BARCs with the resist. We have observed, for example, that a large underexposure margin can occur with samples that have some footing present at the base of the resist, while undercut can induce early line collapse and small underexposure margin. Nevertheless, all things being equal, surface energy matching seems to play a role on lithographic performance using the NTD process.

We found that a more challenging approach was direct patterning on a silicon-containing hardmask. Initial attempts produced severe line collapse (Figure 5). The SCA of the hardmask used was 84° while the resist measured 59° (after exposure and PEB). The failure mode during patterning was attributed to the large differential in surface energy between the silicon hardmask and the resist. Cross-sectional SEM analysis revealed that the lines appear to lift off the surface without having undercut induced line failure (Figure 6).

In order to better understand the role of surface energy on lithographic performance, several samples were prepared having similar silicon content while changing their surface energies by incorporating more polar monomers. A very similar polymer to the one that failed produced good 65-nm trenches just by lowering the SCA by ~ 10° (Figure 5).

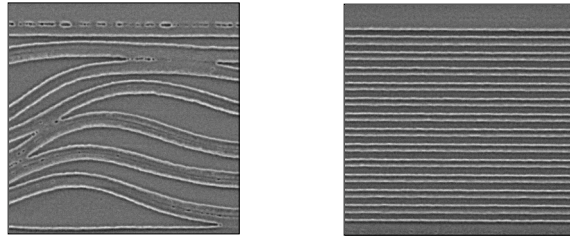


**Figure 5.** Patterning of 65-nm L/S on silicon hardmask with SCA 83° (left) and 72° (right).

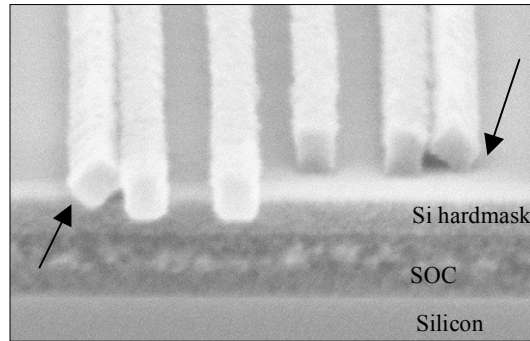


**Figure 6.** Cross-sectional SEM view of line failure showing resist detaching from surface.

### 3.2 Effect of film thickness and reflectivity on lithographic performance

Surface energy matching is an important factor for successful NTD lithography. Consideration of film thickness and reflectivity is equally important. We have found that the same film can perform drastically differently just by changing to a different thickness. For example, let us consider a typical reflectivity curve for a multilayer stack (Figure 7) having a SOC layer 300 nm thick, silicon hardmask, and 90-nm resist (similar to the stack illustrated in Figure 2).

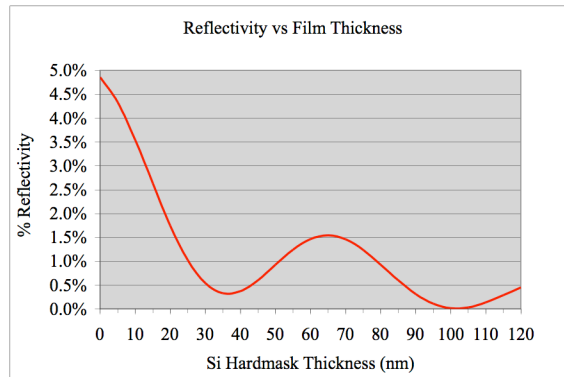


**Figure 7.** Substrate reflectivity versus silicon hardmask thickness (on 300-nm SOC).

The graph in Figure 7 shows that the first reflection minimum occurs at ~ 36 nm (< 0.5%) and the first maximum at ~ 65 nm (1.5%) film thickness. We noticed that even with improved SCA matching, more line collapsed occurred when the silicon hardmask thickness was 36 nm than when a 65-nm thickness was used. In standard PTD processes, best

performance is typically achieved at the first minimum point because less reflection provides better depth of focus and exposure latitude margins. For NTD, this seems to be the opposite, with first maximum being preferred.

In order to explain this observation, we calculated the UV light cross-sectional distribution within the resist at these two reflection points using Brewer Science's OptiStack® modeling software. The UV light cross-sectional distribution is a plot that determines the intensity of light throughout the resist thickness based on the optical properties of the lithographic stack. Figure 8 shows the plot of UV light distribution within the resist. The results show that when a 65-nm silicon hardmask thickness is used, there is more light intensity at the bottom 20 nm of the resist than when the thickness is 36 nm. Because the resist has higher exposure at the lower 20 nm, we could conclude that more acid generation and resist deprotection take place toward the bottom. More acid formation at the bottom has many potential beneficial consequences for minimizing line collapse. For example, a higher level of deprotection could lead to more resistance to solvent developer attack at the resist-hardmask interface. In addition, more acid formation in the resist backbone could act as better anchoring points to the silicon hardmask. Or thirdly, more acid formation at the bottom is usually associated with undercut formation in standard PTD lithography, while with NTD such acid formation could give rise to the reverse behavior – a foot. Foot formation can aid in keeping lines standing.

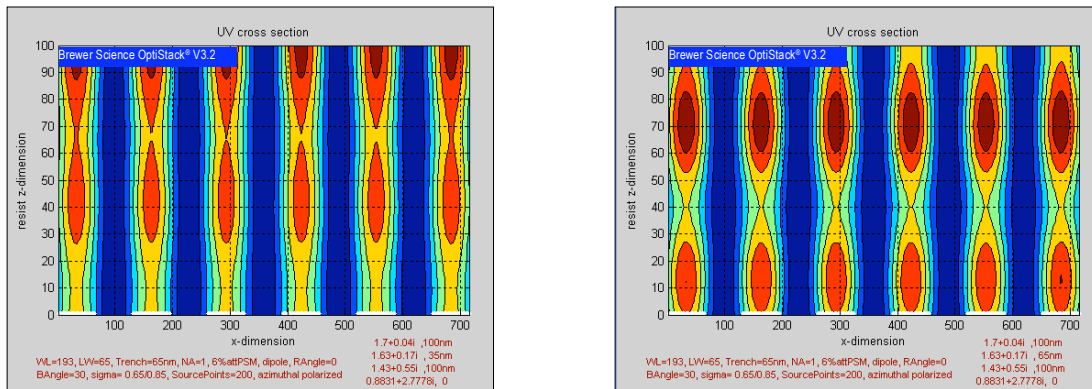


Figure 8. Cross-sectional distribution of UV light intensity within resist at first minimum (left) and first maximum (right).

### 3.3 Effect of spin-on layer composition on lithographic performance

Another effect of interest on the performance of the NTD process is the choice of the SOC used. We have found that the composition of the SOC has a large impact on the resist performance. By using exactly the same silicon hardmask in the stack shown in Figure 2, one can obtain severe line collapse or good patterning just by changing the SOC. This variation in patterning quality implies that the thin silicon hardmask is fairly porous and allows for chemical interaction between the resist and the SOC layer. In this study, we formulated three different underlayers having different pH properties, one with acid components (SOC-A) and one with basic components (SOC-B). The results are shown in Figure 9.

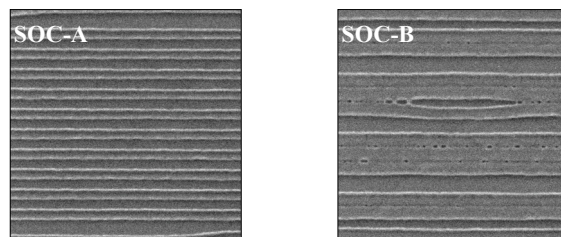


Figure 9. 65-nm L/S patterns obtained using SOC-A and SOC-B with the same silicon hardmask and photoresist.

An explanation for this behavior could be that basic components in the SOC-B layer act to quench the acid generated in the photoresist, which would cause low photoresist deprotection. When the photoresist has low deprotection, it is more

susceptible to attack by solvent developer, causing the lines to collapse. In contrast, the SOC-A layer can act as an acid feed layer that enhances photoresist deprotection and minimizes line collapse.

### 3.4 Lithographic performance

We used the aforementioned knowledge gained regarding surface energy control, thickness, and reflectivity considerations and use of the appropriate SOC layer to evaluate the multilayer stack in a 1900i scanner system. Our target was direct patterning of dense L/S and contact holes using a direct imaging approach (no double patterning of lines). The results for contact holes were not available at the time of manuscript submission. The L/S results collected are shown in Figure 10 below. The dose versus exposure matrix shows the ability to print trenches in the 40- to 60-nm range with a pitch of 104 nm with good exposure and focus latitude. At the edge of the array, pattern collapse or bridging appears to be the main failure mode. A cross-sectional detail from the trenches from relative -0.5mJ dose and 0 $\mu$ m focus is shown in Figure 11.

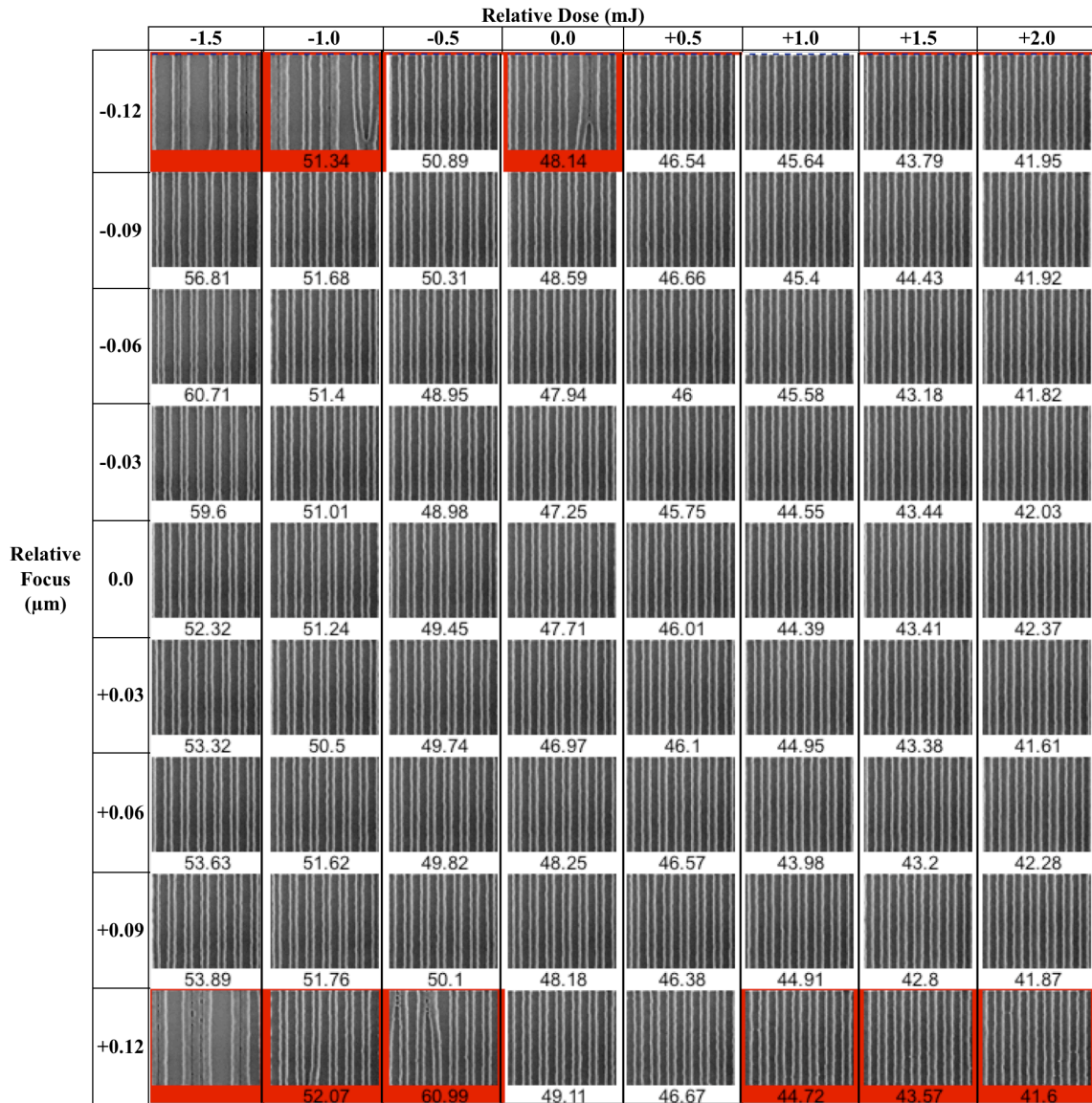
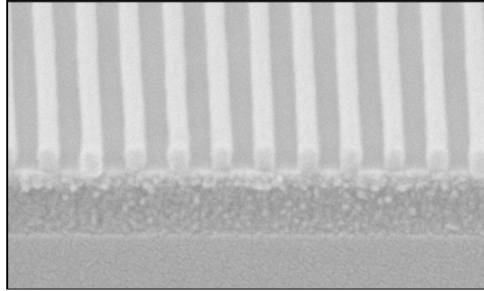


Figure 10. Dose-focus array of dense L/S patterns using NTD process on silicon hardmask substrate.



**Figure 11.** Cross-sectional view of 50-nm trenches, 104-nm pitch patterning, using NTD process on silicon hardmask.

#### 4. CONCLUSIONS

In this study, we investigated the impact that BARC film properties have on the NTD process. The results shown reveal that the surface energy of a BARC or silicon-containing hardmask is a very important factor in controlling line collapse and overall lithographic performance. Even when the surface energy mismatch between the silicon hardmask and the photoresist is minimized, thickness effects (related to overall stack reflectivity) need to be considered. In addition, the composition of the underlying SOC pattern transfer layer can influence the process outcome based on possible diffusion effects occurring throughout the silicon hardmask layer. Finally, when all of these factors are taken into account, successful dense trench patterning can be achieved using the NTD process.

#### ACKNOWLEDGMENTS

The authors would like to thank Mario Reybrouck from FFEM for his assistance and for providing resist materials, Sharon Brown, Jamie Storie, John Thompson, and Denise Howard from Brewer Science for sample preparation and SEM analysis. This work was performed under the IMEC Industrial Affiliation Program.

#### REFERENCES

- [1] S. Tarutani, H. Tsubaki, S. Kamimura, "Materials and Processes of Negative Tone Development for Double Patterning Process," *Journal of Photopolymer Science and Technology*, 22(5), 635-640 (2009).
- [2] S. Tarutani, T. Hideaki, S. Kamimura, "Development of materials and processes for negative tone development toward 32-nm node 193-nm immersion double-patterning process," *Proceedings of SPIE*, 7273, 72730C (2009).
- [3] S. Tarutani, S. Kamimura, J. Yokoyama, "Process parameter influence to negative tone development process for double patterning," *Proceedings of SPIE*, 7639, 76391Q (2010).
- [4] L. Van Look, J. Bekaert, V. Truffert, V. Wiaux, F. Lazzarino, M. Maenhoudt, G. Vandenberghe, Mario Reybrouck, Shinji Tarutani, "Printing the metal and contact layers for the 32- and 22-nm node: comparing positive and negative tone development process," *Proceedings of SPIE*, 7640, 764011 (2010).
- [5] O. Nakayama, T. Fukumoto, M. Tachibana, J. Sato, M. Kitayama, T. Kajiyashiki, "Synthesis and evaluation of novel resist monomers and copolymers for ArF lithography II," *Proceedings of SPIE*, 6923, 69233F (2008).
- [6] D. Guerrero, "Evaluation of Hardmask and BARCs Using Negative Tone Development," FujiFilm Electronic Materials Symposium, Dresden, October 2010.